Reward Prediction for Representation Learning and Reward Shaping

Hlynur Davíð Hlynsson and Laurenz Wiskott
Institut für Neuroinformatik, Ruhr-Universität Bochum, Universitätsstraße 150, Bochum, Germany

Keywords: Reinforcement Learning, Representation Learning, Deep Learning, Machine Learning.

Abstract: One of the fundamental challenges in reinforcement learning (RL) is the one of data efficiency: modern algorithms require a very large number of training samples, especially compared to humans, for solving environments with high-dimensional observations. The severity of this problem is increased when the reward signal is sparse. In this work, we propose learning a state representation in a self-supervised manner for reward prediction. The reward predictor learns to estimate either a raw or a smoothed version of the true reward signal in an environment with a single terminating goal state. We augment the training of out-of-the-box RL agents in single-goal environments with visual inputs by shaping the reward using our reward predictor during policy learning. Using our representation for preprocessing high-dimensional observations, as well as using the predictor for reward shaping, is shown to facilitate faster learning of Actor Critic using Kronecker-factored Trust Region and Proximal Policy Optimization.

1 INTRODUCTION

Deep learning has enjoyed great success in recent years with a fortunate combination of larger data sets, increasing computational capabilities and advances in algorithm design in addition to an ample offering of flexible software ecosystems. In particular, reinforcement learning (RL), which is the discipline of machine learning concerned with general goal-directed behavior. RL has shown great promise since DeepMind combined the principles of RL with deep learning to achieve human-like skill on Atari video games (Mnih et al., 2013). Since then, the list of games where machine triumphs over man grows longer with the addition of algorithms surpassing human capabilities in games such as Go, (Silver et al., 2016), Poker (Brown and Sandholm, 2019) and a restricted version of DOTA 2 (Berner et al., 2019).

Even though the dominance of humans is being tested by RL agents on numerous fronts, there are still great difficulties for the field to overcome. For instance, the data that is required for algorithms to reach human performance is on a far larger scale than that needed by humans. Furthermore, the general intelligence of humans remains unchallenged. Even though an RL agent has reached superhuman performance in one field, its performance is usually poor when it is tested in new areas.

The study of methods to overcome the problem of data efficiency (Hlynsson et al., 2019) and transferability of RL agents in environments where the agent must reach a single goal is the focal point of this work. We consider a simple way of learning a state representation by predicting either a raw or a smoothed version of a sparse reward yielded by an environment. The two objectives, learning a representation and predicting the reward, are directly connected as we train a deep neural network for the prediction and the hidden layers of this network learn a reward-predictive representation of the input data.

The reward signal is created by collecting data from a relatively low number of initial episodes using a controller that acts randomly. The representation is then extracted from an intermediate layer of the prediction model and re-used as general preprocessing for RL agents, to reduce the dimensionality of visual inputs. The agent processes inputs corresponding to its current state as well as the desired end state, which is analogous to mentally visualizing a goal before attempting to reach it. This general approach of relying on state representations, that are learned to predict the reward rather than maximizing it, has been motivated in the literature (Lehnert et al., 2020) and we show that our representation is well-suited for single-goal environments. Our work adds to the growing body of knowledge related to deep unsupervised (Hlynsson

Hlynsson, H. and Wiskott, L.
Reward Prediction for Representation Learning and Reward Shaping.
DOI: 10.5220/0010640200003063
In *Proceedings of the 13th International Joint Conference on Computational Intelligence (IJCCI 2021)*, pages 267-276
ISBN: 978-989-758-534-0; ISSN: 2184-3236

and Wiskott, 2019) and self-supervised (Schüler et al., 2018) representation learning .

We also investigate the effectiveness of augmenting the reward for RL agents, when the reward is sparse, with a novel problem-agnostic reward shaping technique. The reward predictor, which is used to train our representation, is not only used as a part of an auxiliary loss function to learn a representation, but it is also used during training the RL system to encourage the agent to move closer to a goal location. Similar to advantage functions in the RL literature, given the trained reward predictor, the agent receives an additional reward signal if it moves from states with a low predicted reward to states with a higher predicted reward. We find this reward augmentation to be beneficial for our test environment with the largest state-space.

2 BACKGROUND

2.1 Markov Decision Processes

A partially-observable Markov decision process (POMDP) is a tuple

$$(\mathcal{S}, \mathcal{A}, \mathcal{P}, \mathcal{R}, \mathbb{P}(s_0), \Omega, O, \gamma) \tag{1}$$

which we also refer to as the *environment*.

The environment starts in a state $s \in \mathcal{S}$ drawn from $\mathbb{P}(s_0)$, from which the agent interacts sequentially with the environment by choosing action a_t from action space $\mathcal{A}$ at time steps t.

Given the agent's state s_t and action a_t, the transition function $\mathcal{P}$ governs the next state s_{t+1}. The agent receives an observation $o_t \in \Omega$, determined by the observation function O, and a reward r_t, determined by the reward function $\mathcal{R}$.

A discount factor $\gamma \in (0,1)$ is usually included in the definition of POMDPs and it comes into play in the optimization function of the agent. Namely, the objective of an RL agent is to learn a *policy* π that determines the behavior of the agent in the environment by mapping states to a probability distribution over $\mathcal{A}$, written $\pi(a,s) = \mathbb{P}(a_t = a | s_t = s)$. The policy should maximize the expected discounted future sum of rewards, or the expected *return*:

$$R_\Sigma = \sum_{t=0}^{\infty} \gamma^t r_t \tag{2}$$

2.2 Reward Shaping

Sparse rewards in environments is a common problem for RL agents. The agent's goal is to associate its inputs with actions that lead to high rewards, which can be a lengthy process if the agent only rarely experiences positive or negative rewards.

Reward shaping (Mataric, 1994) is a popular method of modifying the reward function of an MDP to speed up learning. It is useful for environments with sparse rewards to augment the training of the agent but skillful applications of reward shaping can in principle aid the optimization for any environment – although the efficacy of the reward shaping is highly dependent on the details of the implementation (Amodei and Clark, 2016). In the last few years, reward shaping has been shown to be useful for complex video game environments, such as real-time strategy games (Efthymiadis and Kudenko, 2013) and platformers (Brys et al., 2014) and it has also been combined with deep neural networks to improve agents in first person shooter games (Lample and Chaplot, 2017).

As an illustration, consider learning a policy for car racing. If the goal is to train an agent to drive optimally, then supplying it with a positive reward for reaching the finish line first is in theory sufficient. However, if it is punished for actions that are never beneficial, for instance crashing into walls, it prioritizes learning to avoid such situtations, allowing it to explore more promising parts of the state space.

Furthermore, just reaching the goal is insufficient if there is competition. To make sure that we have a winning racer, a small negative reward can be introduced at every time step to urge the agent to reach the finish line quickly. Note that the details of the reward shaping in this example requires domain knowledge from a designer who is familiar with the environment. It would be more generally useful if the reward shaping would be autonomously learned, just as the policy of the agent, as we propose to do in this work.

2.3 Reward-predictive/Maximizing Representations

(Lehnert et al., 2020) make the distinction between *reward-maximizing* representations are *reward-predictive* representations. They argue how reward-maximizing representations can transfer poorly to new environments while reward-predictive representations generalize successfully. Take the simple grid world navigation environments in Figure 1, for example. The agent starts at a random tile in the grid and gets a reward of +1 by reaching the rightmost column in Environment A or by reaching the middle column in Environment B. The state space in Environment A can be compressed from the 3×3 grid to a vector of length 3, $[\phi_1^p, \phi_2^p, \phi_3^p]$ of reward-predictive representations. To predict the discounted reward, it suffices to describe the agent's state with ϕ^p_j if it is in the jth row.

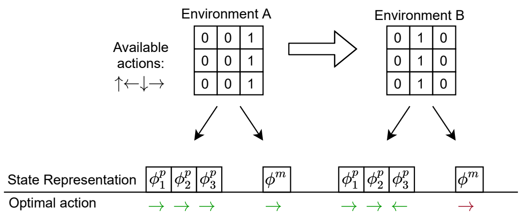

Figure 1: **Reward-maximizing vs. reward-predictive representations**. In this grid world example, the agent starts the episode at a random location and can move up, down, left, or right. The episode ends with a reward of 1 and terminates when the agent reaches the rightmost column. Both the reward-predictive representation and reward-maximizing representation ϕ^p and ϕ^m, respectively, are useful for learning the optimal policy in Environment A. The reward-predictive representation ϕ^p collapses each column into a single state to predict the discounted future reward. The reward-maximizing representation ϕ^m makes no such distinction as moving right is the optimal action in any state. It is a different story if the representations are transfered to Environment B, where reaching the middle column is now the goal. The representation ϕ^p can be reused and the optimal policy is found if agent now takes a step left in ϕ^p_3. However, the representation ϕ^m is unable to discriminate between the different states and is useless for determining the optimal policy.

The reward-maximizing representation for Environment A is much simpler: the whole state space can be collapsed to a single element ϕ^m, with the optimal policy of always moving to the right. If these representations are kept, then the reward-predictive representation ϕ^p is informative enough for a RL agent to learn how to solve Enviroment B. The reward-maximizing representation ϕ^m has discarded too many details of the environment to be useful for solving this new environment.

2.4 Successor Features

The *successor representation* algorithm learns two functions: the expected reward R^{SF}_π received after transitioning into a state s, as well as the matrix M^{SF}_π of discounted expected future occupancy of each state, assuming that the agent starts in a given state and follows a particular policy π. Knowing the quantities R^{SF}_π and M^{SF}_π allows us to rewrite the value function:

$$V_\pi(s) = \mathbb{E}_{s'}\left[R^{\text{SF}}_\pi(s) M^{\text{SF}}_\pi(s,s')\right] \tag{3}$$

The motivation for this algorithm is that it combines the speed of model-free methods, by enabling fast computations of the value function, with the flexibility of model-based methods for environments with changing reward contingencies.

This method is made for small, discrete environments but it has been generalized for continuous environments with so-called feature-based successor representations, or *successor features* (SFs) (Barreto et al., 2016). The SF algorithm similarly calculates the discounted expected representation of future states, given the agent takes the action a in the state s and follows a policy π:

$$\psi_\pi(s,a) = \mathbb{E}_\pi\left[\sum_{t=0}^{\infty} \gamma^{t-1}\phi_{t+1} | s_t = s, a_t = a\right] \tag{4}$$

where ϕ is some state representation. Both the SF ψ and the representation ϕ can be deep neural networks.

3 RELATED WORK

3.1 Reward-predictive Representations

(Lehnert et al., 2020) compare successor features (SFs) to a nonparametric Bayesian predictor that is trained to learn transition and reward tables for the environment, either with a reward-maximizing or a reward-predictive loss function. (Lehnert and Littman, 2020) prove under what conditions successor features (SFs) are either *reward-predictive* or *reward-maximizing* (see distinction in Section 2.3). They also show that SFs work succesfully for transfer learning between environments with changing reward functions and unchanged transition functions, but they generalize poorly between environments where the transition function changes.

Our work is distinct from the reward-predictive methods that they compare as our representation does not need to calculate expected future state occupancy, as is the case for SFs. Our method scales better for more complicated state-spaces because we do not tabulate the states, as they do with their Bayesian model, but learn arbitrary continuous features of high-dimensional input data. In addition to that, learning our reward predictor is not only a "surrogate" objective function as we use it for reward shaping as well.

3.2 Reward Shaping

The advantages of reward shaping are well understood in the literature (Mataric, 1994). A recent trend in RL research is the study of methods that can learn the reward shaping function in an automatic manner, without the need of (often faulty) human intervention.

(Marashi et al., 2012) assume that the environment can be expressed as a graph and that this graph formulation is known. Under these strong assumptions, they perform graph analysis to extract a reward shaping function. More recently, (Zou et al., 2019) propose a meta-learning algorithm for potential-based automatic reward shaping. Our approach is different from previous work as we assume no knowledge about the environment and train a predictor to approximate (potentially smoothed) rewards, which is then used to construct a potential-based reward shaping function.

3.3 Goal-conditioned RL

(Kaelbling, 1993) studied environments with multiple goals and small state-spaces. In their problem setting, the agent must reach a known but dynamically changing goal in the fewest number of moves. The observation space is of a low enough dimension for dynamic programming to be satisfactory in their case. (Schaul et al., 2015) introduce the Universal Value Function Approximators and tackle environments of larger dimensions by learning a value function neural network approximator that accepts both the current state and a goal state as the inputs. In a similar vein, (Pathak et al., 2018) learn a policy that is given a current state and a goal state and outputs an action that bridges the gap between them. (Hlynsson et al., 2020) learn a predictable representation that is paired with a representation predictor and combine it with graph search to find a given goal location. In contrast to these approaches, we learn a reward-predictive representation in a self-supervised manner which is used to preprocess raw inputs for RL policies.

4 APPROACH

In this section, we explain our approach mathematically. Intuitively, we train a deep neural network to predict either a raw or a smoothed reward signal from a single-goal environment. The output of an intermediate layer in the network is then extracted as the representation – for example, by simply removing the top layers of the network. The full reward predictor network is used for reward shaping by rewarding the agent for moving from lower predicted values toward higher predicted values of the network.

4.1 Learning the Representation

Suppose that $f_\theta : \mathbb{R}^c \to [0,1]$ is a differentiable function parameterized by θ and c is a positive integer. We use f_θ to approximate the discounted return in a POMDP with a sparse reward: the agent receives a reward of 0 for each time step except when it reaches a goal location, at which point it receives a positive reward and the episode terminates.

Given an experience buffer $\mathcal{D} = \{(s_t, a_t, r_t, s_{t+1})_i\}$, we create a new data set $\mathcal{D}^* = \{(s_t, a_t, r_t^*, s_{t+1})_i\}$. The new rewards are calculated according to the equation

$$r_t^* = \gamma^m r_{t+m} \tag{5}$$

where $\gamma \in [0,1]$ is a discount factor and $M > m > 0$ is the difference between t and the time step index of the final transition in that episode, for some maximum time horizon M. Throughout our experiments, we keep the value of the discount factor equal to 0.99 and we train on $\mathcal{D}$ or $\mathcal{D}^*$.

Assume that our differentiable representation function $\phi : \mathbb{R}^d \to \mathbb{R}^c$ is parameterized by θ' and maps the d-dimensional raw observation of the POMDP to the c-dimensional feature vector. We train the representation for the discounted-reward prediction by minimizing the loss function

$$\mathcal{L}(f_\theta[\phi_{\theta'}(s_{t+1})], r_t^*) = (r_t^* - f_\theta[\phi_{\theta'}(s_{t+1})])^2 \tag{6}$$

with respect to the parameters θ of f and the parameters θ' of ϕ over the whole data set $\mathcal{D}^*$. See Figure 2 for a conceptual overview of our representation learning.

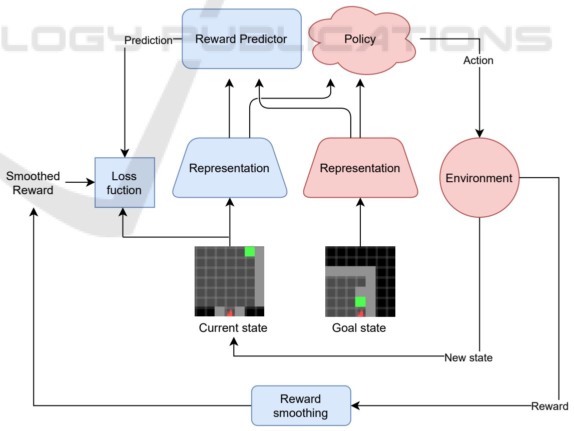

Figure 2: **Learning and Using the Representation.** Our representation and reward predictor is trained with the elements highlighted in blue. The trained representation is then used for dimensionality reduction for an RL agent, that interacts with the environment as indicated by the elements highlighted in red.

4.2 Reward Shaping

(Ng et al., 1999) define a reward shaping function F as *potential-based* if there exists a function $f : \mathcal{S} \to \mathbb{R}$ such that for all states $s, s' \in \mathcal{S}$ the equation holds:

$$F(s,a,s') = \gamma f(s') - f(s) \tag{7}$$

and γ is the MDP's discount factor. They prove for single-goal environments that every optimal policy for the MDP $M = (\mathcal{S},\mathcal{A},\mathcal{P},\mathcal{R},\mathbb{P}(s_0),\gamma)$ is also optimal for its reward-shaped counterpart $M' = (\mathcal{S},\mathcal{A},\mathcal{P},\mathcal{R}+F,\mathbb{P}(s_0),\gamma)$, and vice versa. They also show, for a given state space $\mathcal{S}$ and action space $\mathcal{A}$, that if F is not potential-based, then there exist a transition function $\mathcal{P}$ and a reward function $\mathcal{R}$ such that no optimal policy in M' is optimal in M.

We would like our reward shaping function to be potential-based (Equation 7) to reap the theoretical advantages and propose a potential-based reward shaping function based on the reward predictor

$$\begin{aligned} F(s,a,s') &= \left(\gamma f_\theta(\phi_{\theta'}[s']) - f_\theta(\phi_{\theta'}[s])\right)(H-I)/H \\ &= \gamma f^*(s') - f^*(s) \end{aligned} \tag{8}$$

where $f^* = f_\theta(\phi_{\theta'}[s'])(H-I)/H$, f_θ is the reward predictor and $\phi_{\theta'}$ is our representation from the previous section. Note that both f_θ and $\phi_{\theta'}$ are assumed to be fully trained before the policy of the agent is trained, for example using data gathered by a random policy, but they can in principle also be updated as the policy is being learned. The factor $(H-I)/H$ scales down the intensity of the reward shaping where $I \in \mathbb{N}^+$ is the number of episodes that the agent has experienced and $H \in \mathbb{N}^+$ is the maximum number of episodes where the agent is trained using reward shaping. The strength of the reward shaping is the highest in the beginning to counteract potentially adverse effects of errors in the reward predictor. It is also more important to incentivize moving toward the general direction of the goal in the early stages of learning, after which the un-augmented reward signal of the environment is allowed to "speak for itself" and guide the learning of the agent toward the goal precisely.

5 METHODOLOGY AND IMPLEMENTATION

5.1 Environment

The method is tested on 3 different gridworld environments based on the Minimalistic Gridworld Environment (MiniGrid) (Chevalier-Boisvert et al., 2018). Tiles can be empty, occupied by a wall or occupied by lava. The constituent states of $\mathcal{S}$ are determined by the agent's location and direction (facing north, west, south or east), along with the goal's location. The steps taken since the episode's initialization is also tracked for reward calculations. See Figure 3a for 3 different world states in one of our environments.

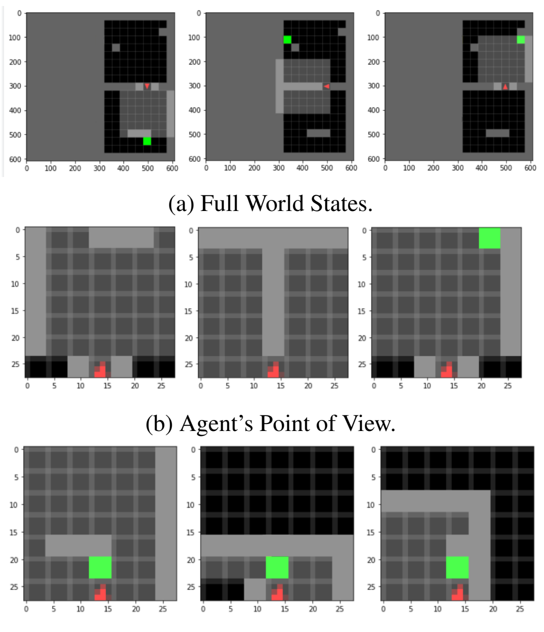
(a) Full World States.

(b) Agent's Point of View.

(c) Goal Observations.

Figure 3: **Two-Room Environment.** The red agent must reach the green goal in as few steps as possible. The agent starts each episode between the two rooms, facing a random direction (up, down, left or right). Each column corresponds to a snapshot of 1 episode. The light tiles correspond to what the agent sees while the dark tiles are unseen by the agent. (a) Examples of the full state (b) The observation from the agent's current state (c) A goal observation. This is the agent's point of view from a state that separates the agent from the goal by 1 action.

The action space $\mathcal{A}$ has 3 actions: (1) turn left, (2) turn right and (3) move forward. The transition function is deterministic. The agent relocates to the tile it faces if it moves forward and the tile is empty and nothing happens if the tile is occupied by a wall. The episode terminates if the tile is occupied by lava or the goal. The agent rotates in place if it turns left or right. Reaching the green tile goal gives a reward of $1 - 0.9 \cdot \frac{\#\text{steps taken}}{\#\text{max steps}}$, other actions give no reward. The environment times out after #max step $= 100$ steps. The discount factor is $\gamma = 0.99$.

We consider the following three environments:

5.1.1 Two-room Environment

The world is a 8×17 grid of tiles, split into two rooms, where walls are placed at different locations to facilitiate discrimination between the rooms from the agent's point of view. (Figure 3). The agent is placed between the two rooms, facing a random direction. The goal is at 1 of 3 possible locations. This is a modified version of the classical four-room environment layout (Sutton et al., 1999).

5.1.2 Lava Gap Environment

In this environment, the agent is in a 4×4 room with a column of lava either 1 or 2 spaces in front of the agent (Figure 4) with a gap in a random row. The agent always starts in the upper left corner and the goal is always in the lower right corner.

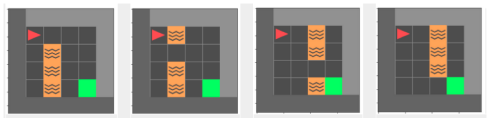
Figure 4: **The Lava Gap Environment.** The red agent must reach the green goal in as few steps as possible while avoiding the orange lava tiles.

5.1.3 Four-room Environment

An expansion to the two-room environment with two additional rooms (Figure 5) and both the agent and the goal location are placed at random locations.

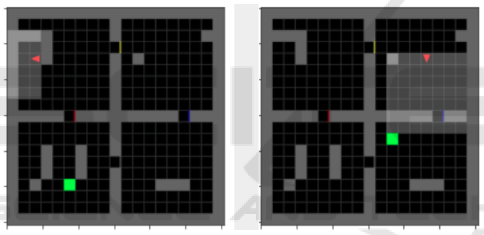
Figure 5: **Four-Room Environment**. The agent and goal locations are randomized in each episode. The 7×7 grid of highlighted tiles in front of the agent is the observation.

5.2 Baselines

We combine our representations with two RL algorithms as implemented in Stable Baselines (Hill et al., 2018) using the default hyperparameters: (1) Actor Critic using Kronecker-Factored Trust Region (ACKTR) (Wu et al., 2017) and a version of the Proximal Policy Optimization (PPO2) algorithm (Schulman et al., 2017).

For both algorithms, 6 variations are compared: (1) ACKTR / PPO2 with raw image inputs (Deep RL), (2) inputs are preprocessed with successor features (SF), (3) inputs are preprocessed using our representation, trained on raw reward predictions (Ours 1r), (4) the input is preprocessed using our representation and the reward is shaped, trained on raw reward predictions (Ours 1r + Shaping), (5) the input is preprocessed using our representation, trained on smoothed reward predictions (Ours 64r), (6) the input is preprocessed using our representation and the reward is shaped, trained on smoothed reward predictions (Ours 64r + Shaping). Care has been taken to ensure that each model has the same architecture and number of parameters.

5.3 Model Architectures

Every model is realized as a neural network using Keras (Chollet et al., 2015). Below, the representation and policy networks are used for our method and the SF comparison, the reward prediction network is used only for our method and the deep RL network is used only for the deep RL comparison, where the RL algorithm also learns the representation.

The Representation Networks: are two convolutional networks with a $28 \times 28 \times 3$ input. The first layer discards every other column and row. This is followed by 8 filters of size 3×3 with a stride of 3. This is followed with a ReLU activation and a 2×2 max pooling layer with a stride of 2. The pooling layer's output is passed to a layer with 16 convolutional filters of size 3×3 and a stride of 2 and a ReLU activation. The output is passed to a linear dense layer with 16 units, defining the dimension of the representation. No zero padding is applied in any layer.

The Policy Networks: are 3-layer fully-connected networks accepting the concatenated output of the representation network for the agent's current point of view and the goal observation as input. The first two layers have 64 units and a ReLU activation and the last layer has 3 units and a linear activation function. The three units represent the three actions left, right, and forward in a one hot encoding. Winner takes all is used to decide on the action.

Our Reward Prediction Network: is a 3-layer fully-connected network with the same input as the policy network: the concatenated representation of the agent's current view and the goal observation. The first two layers have 256 units and a ReLU activation but the last layer has 1 unit and a logistic activation.

The Deep RL Network: stacks the representation network and the policy network on top of each other. The representation network accepts the input and outputs the low-dimensional representation to the policy network that outputs the action scores.

5.4 Training the Representation and Predictor Networks

We collect a data set of 10 thousand transitions by following a random policy in the two-room environment. For this data collection, each episode has a 50%

chance to have the goal location in the bottom room or on the left side of the top room (see the left and middle pictures in Figure 3a). The reward predictor and the representation are trained in this manner for all experiments, including the lava gap and the four-room environment. Thus, we use a representation and reward predictor that have never seen lava. For the experiments with smoothed rewards, the sparse reward associated with the observations in the data set is augmented by associating a new reward to the 64 states leading to observations with a positive reward using Equation 5 with a discount factor of 0.99. Ater the reward has been (potentially) smoothed in this way, observations associated with a positive reward are oversampled 10 times to balance the data set, regardless of whether the reward has been augmented or not.

6 RESULTS AND DISCUSSION

6.1 Two-room Environment

We start by visualizing the outputs of our reward predictor in the rooms, depending on the goal location, in Figure 6. Each square indicates the average predicted reward for transitioning to the corresponding tile.

The predicted reward spikes in a narrow region around the two goal locations that were used to train the raw reward predictor (Figure 6a), but the area of states with high predicted rewards is wider around the test goal. This difference is due to overfitting on the specific training paths that were more frequently taken toward the respective goals, but this does not harm the generalization capabilities of the network. The peakyness of the predictions disappears when the predictor is trained on the smoothed rewards (Figure 6b). However, higher predicted rewards in the corner of the other room appear. Both scenarios, raw and smoothed reward prediction, show promise for the application of reward shaping under our training scheme, as the agent benefits from finding neighborhoods with higher values of predicted reward until it reaches the goal, instead of relying on a sparse reward that is only given when the agent lands on the goal.

In Figure 7, we illustrate the variance of the mean reward (left side) and the variance of the optimal performance (right side) of the different methods, as a function of the time steps taken for training. We average over 10 runs and in each run we perform 10 test rollouts, so each point is the aggregate of 100 episodes in total. The error bands indicate two standard deviations. This methodology of generating the plots also applies to Figure 9, Figure 10 and Figure 11.

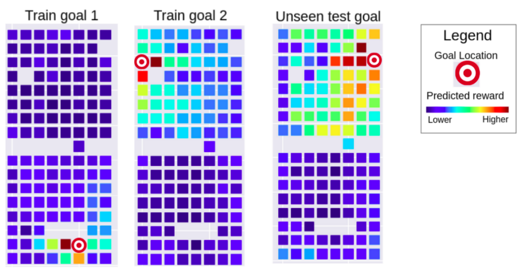

(a) Raw reward prediction.

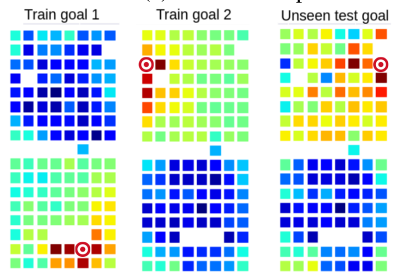

(b) Smoothed reward prediction.

Figure 6: **Predicted Rewards, Two-room environment.** The predictor is trained on the setups shown on the left and in the middle, and tested for the setup on the right.

The learning curves of ACKTR and PPO2 get close to a mean reward of 1 the fastest using our representations. There no significant benefit from using smoothed reward shaping for ACKTR, and the raw reward shaping is in fact harmful in this case. For PPO2, the agent using our representation that is trained on raw reward predictions learns the fastest. Regular deep RL is clearly outperformed by the variants that use reward-predictive representations. We believe that this is because RL agents can generally benefit from the input being preprocessed, as the computational overhead for learning the policy is reduced. This effect is enhanced when the preprocessing is good, which is the case for our representation: it abstracts away unnecessary information as it trained to output features that indicate the distance between the agent and the goal, when the goal is in view.

The difference in the performance of a method on the left hand side vs. the right hand side can be explained due to systematically different behaviors. For example, an agent might be poor at searching for the goal, giving it low average mean rewards, but it takes the direct course to the goal when it sees it, giving it a good average minimum episode length.

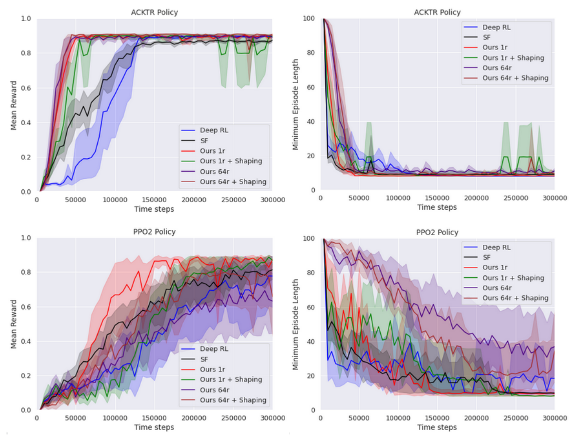

Figure 7: **Two-room Environment**. In these experiments, there are only two rooms and the agent must reach a goal that is always at the same location.

6.2 Lava Gap Environment

6.2.1 Learning from Scratch

The heatmaps of average predicted rewards are visualized in Figure 8. The reward predictor was trained on the two-room environment. The tiles closest to the goal have the highest values, with a particularly smooth gradient toward the goal for the smoothed-reward predictor, which demonstrates that there is potential gain from transfering the prediction-based reward shaping between similar environments. The learning performance of the different methods can be seen in Figure 9. The decidedly fastest learning can be observed when the actor-critic method is combined with our representation, trained on raw reward predictions and without reward shaping. Regular deep RL is the second-best but with a very large variance on the performance. Our reward shaping variations and the SFs are very close in performance, albeit significantly worse than the other two. The poor performance of reward shaping can be explained by the fact that there are very few states, which makes the reward shaping unnecessary in such a simple environment. All the methods look more similar when PPO2 optimization is applied, with respect to the mean rewards, but our variant that is trained on smooth reward prediction and uses reward shaping reaches the highest average performance in the last iterations.

6.2.2 Transfer Learning

To investigate how the methods compare for adapting to new environments, we trained the policies for 8000 steps on the two-room environment before learning to solve the lava gap environment, see Figure 10. Our

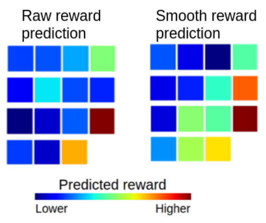

Figure 8: **Predicted Rewards, Lava Gap**. Average predicted reward per state in the lava gap environment.

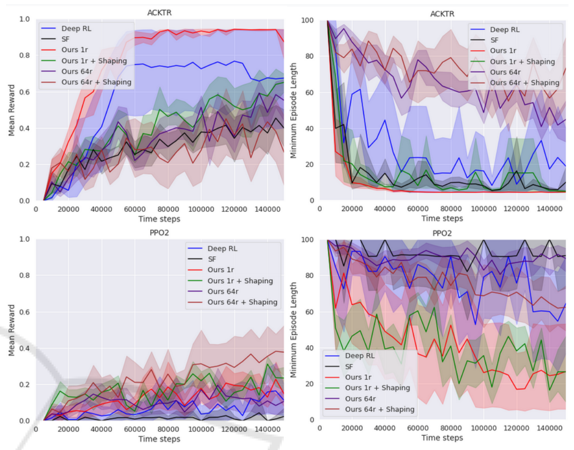

Figure 9: **Lava Gap Experiment.** All policies learn to solve the lava gap environment from scratch.

method, without reward shaping, facilitates the fastest learning for ACKTR in this case. Deep RL is the most severely affected by this change, which is probably due to the method learning a reward-maximizing representation in one environment that does not transfer well to another environment. Every PPO2 variation looks bad for this scenario, but smooth-reward prediction representation with reward shaping has the highest mean reward and our raw-reward prediction representation has the lowest average minimum episode length.

6.3 Four-room Environment

In our final comparison, we add two additional rooms to the two-room environment and randomize both the goal location and the starting position of the agent, with the results shown in Figure 11. Looking at the minimum episode lengths, for the ACKTR learner, our raw-reward prediction representation with reward shaping performs best and the one without reward shaping comes in second. There is little discernible difference between the performance of SFs and Deep RL, but they both perform significantly worse than our methods. The scale of the mean reward is a great deal lower than in the previous experiments since the

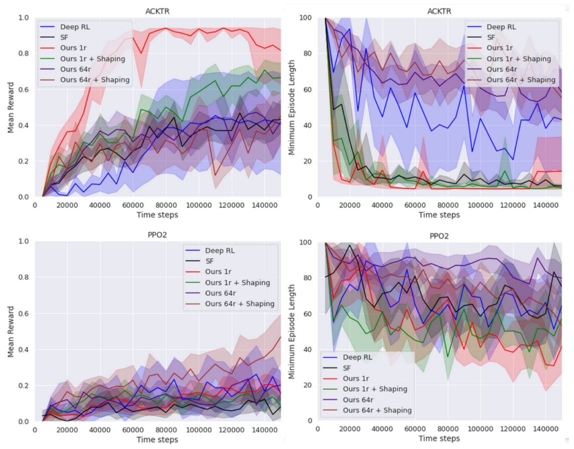

Figure 10: **Re-learning Experiment** The policies are trained for 8 thousand training steps on the two-room environment before being trained on the lava gap environment.

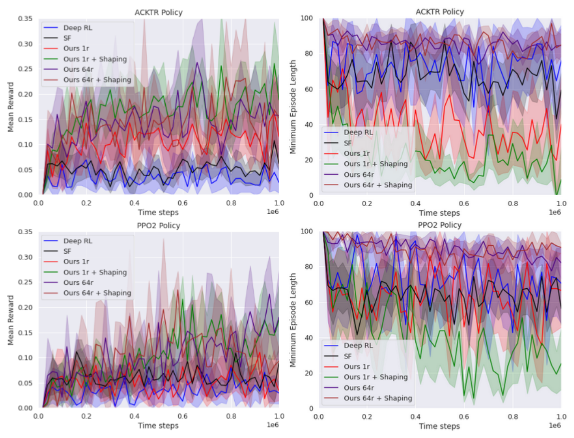

Figure 11: **Full Four-room Environment**. The agent and goal are placed at random locations at the start of each episode.

average distance between the starting tile of the agent and the goal is much larger than in the previous two environments.

For this scenario, all the methods look similarly bad for the PPO2 policy, except for our raw-reward representations, with reward shaping, which has the lowest minimum episode length. The big advantage of reward shaping in this environment compared to the two-room environment can be explained by the increased complexity, making the reward shaping more helpful in guiding the agent's search. In the previous experiments, the agent and goal locations start at fixed locations, allowing the agents to solve it by rote memorization. The reward shaping function calculated by the raw-reward predictor fares significantly better in this situation. We hypothesize that this is due to the smoothed-reward predictor distracting the agent by pushing it to corners, as the visualization in Figure 6b would suggest.

The reward shaping given by the raw-reward predictor is more discriminative, as we see in Figure 6a. The agent receives a positive reward as soon as the goal reaches its point of view, which is any location up to 6 tiles in front of it and no further than 3 tiles away from it to the left or to the right. This allows the reward shaping function to guide the agent directly to the goal, assuming that they are in the same room and that there is no wall obstructing the agent's field of vision.

7 CONCLUSION

Processing high-dimensional inputs for reinforcement learning agents remains a difficult problem, especially if the agent must rely on a sparse reward signal to guide its representation learning. In this work, we put forward a method to help alleviate this problem with a method of learning representations that preprocesses visual input for reinforcement learning (RL) methods. Our contributions are (i) a reward-predictive representation that is trained simultaneously with a reward predictor and (ii) a reward shaping technique using this trained predictor. The predictor learns to approximate either the raw reward signal or a smoothed version of it and it is used for reward shaping by encouraging the agent to transition to states with higher predicted rewards.

We used a view of the goal as a second input for the methods in our experiments, but this is in principle not necessary as moving toward the green tile as it becomes visible is sufficient. Removing the goal input might encourage the agents to learn policies that scan all the rooms faster until the goal reaches its field of vision.

We have shown the usefulness of our representation and our reward shaping scheme in a series of gridworld experiments, where the agent receives a visual observation of its goal as input along with an observation of its immediate surroundings. Preprocessing the input using this representation speeds up the training of two out-of-the-box RL methods, Actor Critic using Kronecker-Factored Trust Region and Proximal Policy Optimization, compared to having these methods learn the representations from scratch. In our most complicated experiment, combining our representation with our reward shaping technique is shown to perform significantly better than the vanilla RL methods, which hints at its potential for success, especially in more complex RL scenarios.

ACKNOWLEDGEMENT

We would like to thank Moritz Lange for his valuable contribution to the preparation of this paper.

REFERENCES

Amodei, D. and Clark, J. (2016). Faulty reward functions in the wild. https://blog.openai.com/faulty-reward-functions/,2016.

Barreto, A., Dabney, W., Munos, R., Hunt, J. J., Schaul, T., Van Hasselt, H., and Silver, D. (2016). Successor features for transfer in reinforcement learning. *arXiv preprint arXiv:1606.05312*.

Berner, C., Brockman, G., Chan, B., Cheung, V., Dębiak, P., Dennison, C., Farhi, D., Fischer, Q., Hashme, S., Hesse, C., et al. (2019). Dota 2 with large scale deep reinforcement learning. *arXiv preprint arXiv:1912.06680*.

Brown, N. and Sandholm, T. (2019). Superhuman ai for multiplayer poker. *Science*, 365(6456):885–890.

Brys, T., Harutyunyan, A., Vrancx, P., Taylor, M. E., Kudenko, D., and Nowé, A. (2014). Multi-objectivization of reinforcement learning problems by reward shaping. In *2014 international joint conference on neural networks (IJCNN)*, pages 2315–2322. IEEE.

Chevalier-Boisvert, M., Willems, L., and Pal, S. (2018). Minimalistic gridworld environment for openai gym. https://github.com/maximecb/gym-minigrid.

Chollet, F. et al. (2015). Keras. https://keras.io.

Efthymiadis, K. and Kudenko, D. (2013). Using plan-based reward shaping to learn strategies in starcraft: Broodwar. In *2013 IEEE Conference on Computational Inteligence in Games (CIG)*, pages 1–8. IEEE.

Hill, A., Raffin, A., Ernestus, M., Gleave, A., Kanervisto, A., Traore, R., Dhariwal, P., Hesse, C., Klimov, O., Nichol, A., Plappert, M., Radford, A., Schulman, J., Sidor, S., and Wu, Y. (2018). Stable baselines. https://github.com/hill-a/stable-baselines.

Hlynsson, H. D., Schüler, M., Schiewer, R., Glasmachers, T., and Wiskott, L. (2020). Latent representation prediction networks. *arXiv preprint arXiv:2009.09439*.

Hlynsson, H. D. and Wiskott, L. (2019). Learning gradient-based ica by neurally estimating mutual information. In *Joint German/Austrian Conference on Artificial Intelligence (Künstliche Intelligenz)*, pages 182–187. Springer.

Hlynsson, H. D., Wiskott, L., et al. (2019). Measuring the data efficiency of deep learning methods. *arXiv preprint arXiv:1907.02549*.

Kaelbling, L. P. (1993). Learning to achieve goals. In *IJCAI*, pages 1094–1099. Citeseer.

Lample, G. and Chaplot, D. S. (2017). Playing fps games with deep reinforcement learning. *Proceedings of the AAAI Conference on Artificial Intelligence*, 31(1).

Lehnert, L. and Littman, M. L. (2020). Successor features combine elements of model-free and model-based reinforcement learning. *Journal of Machine Learning Research*, 21(196):1–53.

Lehnert, L., Littman, M. L., and Frank, M. J. (2020). Reward-predictive representations generalize across tasks in reinforcement learning. *PLoS computational biology*, 16(10):e1008317.

Marashi, M., Khalilian, A., and Shiri, M. E. (2012). Automatic reward shaping in reinforcement learning using graph analysis. In *2012 2nd International eConference on Computer and Knowledge Engineering (ICCKE)*, pages 111–116. IEEE.

Mataric, M. J. (1994). Reward functions for accelerated learning. In *Machine learning proceedings 1994*, pages 181–189. Elsevier.

Mnih, V., Kavukcuoglu, K., Silver, D., Graves, A., Antonoglou, I., Wierstra, D., and Riedmiller, M. (2013). Playing atari with deep reinforcement learning. *arXiv preprint arXiv:1312.5602*.

Ng, A. Y., Harada, D., and Russell, S. (1999). Policy invariance under reward transformations: Theory and application to reward shaping. In *Icml*, volume 99, pages 278–287.

Pathak, D., Mahmoudieh, P., Luo, G., Agrawal, P., Chen, D., Shentu, Y., Shelhamer, E., Malik, J., Efros, A. A., and Darrell, T. (2018). Zero-shot visual imitation. In *Proceedings of the IEEE Conference on Computer Vision and Pattern Recognition Workshops*, pages 2050–2053.

Schaul, T., Horgan, D., Gregor, K., and Silver, D. (2015). Universal value function approximators. In *International conference on machine learning*, pages 1312–1320.

Schüler, M., Hlynsson, H. D., and Wiskott, L. (2018). Gradient-based training of slow feature analysis by differentiable approximate whitening. *arXiv preprint arXiv:1808.08833*.

Schulman, J., Wolski, F., Dhariwal, P., Radford, A., and Klimov, O. (2017). Proximal policy optimization algorithms. *arXiv preprint arXiv:1707.06347*.

Silver, D., Huang, A., Maddison, C. J., Guez, A., Sifre, L., Van Den Driessche, G., Schrittwieser, J., Antonoglou, I., Panneershelvam, V., Lanctot, M., et al. (2016). Mastering the game of go with deep neural networks and tree search. *nature*, 529(7587):484–489.

Sutton, R. S., Precup, D., and Singh, S. (1999). Between mdps and semi-mdps: A framework for temporal abstraction in reinforcement learning. *Artificial intelligence*, 112(1-2):181–211.

Wu, Y., Mansimov, E., Grosse, R. B., Liao, S., and Ba, J. (2017). Scalable trust-region method for deep reinforcement learning using kronecker-factored approximation. In *Advances in neural information processing systems*, pages 5279–5288.

Zou, H., Ren, T., Yan, D., Su, H., and Zhu, J. (2019). Reward shaping via meta-learning. *arXiv preprint arXiv:1901.09330*.